GPS DELAY TIME AT LOW LATITUDE DURING SEVERE GEOMAGNETIC STORM

Thanapon Keokhumcheng[1], Nitipat Buakao[1], and Chollada Pansong[2*]
E-mail: kthanaponok@gmail.com[1], 66036079@kmitl.ac.th[1], and collada_p@rmutt.ac.th[2*]

Received: September 20, 2024
Revised: October 25, 2024
Accepted: November 22, 2024

ABSTRACT

This study examines the impact of geomagnetic storms on Total Electron Content (TEC) variations and GPS signal delays in low-latitude regions, focusing on the March 24, 2023 (Dst = -163 nT, Kp = 8), and April 24, 2023 (Dst = -213 nT, Kp = 8) geomagnetic storms. Both events, classified as strong geomagnetic storms, significantly affected ionospheric conditions and GNSS signal propagation, particularly in Thailand. The analysis utilized TEC data from three GNSS stations (THCP in Chumphon, THBK in Bangkok, and THCM in Chiang Mai) and revealed substantial fluctuations in TEC and GPS signal delays during the storms. The results indicate that GPS signal delay times increased significantly on the storm days, peaking on March 24 and April 24, before gradually decreasing during the recovery phase. On March 24, 2023, the highest time delay was observed at THBK (10.70 ns), followed by THCP (10.43 ns) and THCM (9.27 ns), whereas on April 24, 2023, the maximum time delay occurred at THCP (9.59 ns), followed by THBK (9.56 ns) and THCM (9.85 ns) respectively.

Keywords: TEC, Delay time, Geomagnetic storm

*Corresponding author E-mail: kthanaponok@gmail.com
[1]Department of Engineering Education, School of Industrial Education and Technology,
King Mongkut's Institute of Technology Ladkrabang, Bangkok 10520 Thailand
[2*]Department of Technical Education, Faculty of Technical Education, Rajamangala University of Technology Thanyaburi,
Pathum Thani, 12110 Thailand

I. INTRODUCTION

The ionosphere is the uppermost layer of Earth's atmosphere, beginning at approximately 60 km in altitude, where solar extreme ultraviolet (EUV) radiation induces partial ionization (Verkhoglyadova et al., 2021, pp. 1-12). This atmospheric layer responds dynamically to solar and terrestrial disturbances, including space weather events. As a crucial transmission medium, the ionosphere significantly affects Global Navigation Satellite System (GNSS) signals, primarily by introducing delays due to variations in plasma characteristics. These disturbances negatively impact GNSS accuracy and reliability in positioning. Free electrons within the ionosphere play a key role in modifying signal properties. Variationsis phase and amplitude are influenced by the Total Electron Content (TEC), which contributes to both signal delays and phase shifts in GNSS transmissions. When plasma is embedded with a magnetic field, it transfers energy into Earth's atmospheric system, leading to noticeable fluctuations in ionospheric parameters such as TEC and the critical frequency of the F2 layer (foF2). These fluctuations manifest as either positive or negative ionospheric storms, depending on whether electron density increases or decreases over a specific period (Zhang et al., 2020, pp. 86-94). During geomagnetic storms, enhanced currents and the influx of high-energy particles generate significant thermal energy within the ionosphere. This heating effect alters atmospheric density, redistributes particles, and increases drag on satellites in low-Earth orbit. The lower-latitude ionosphere exhibits unique variations, including equatorial ionization anomalies and the formation of equatorial plasma bubbles, which pose challenges for ground-based space systems, particularly GNSS and communication technologies (Marini-Pereira et al., 2020, pp. 1-16). The intensification of ionospheric disturbances is driven by factors such as changes in thermospheric wind patterns, ionospheric motion dynamics, and electric fields, all of which contribute to increased electron density. Conversely, adverse storm effects primarily result from alterations in ionospheric composition (Serafimov et al., 1982, pp. 397-399; Chinmaya et al., 2016, pp. 7941-7960; Reddybattula et al., 2019, pp. 283-292). These geomagnetic disturbances lead to fluctuations in TEC, disrupting satellite signal reception and causing delays in signal transmission. Reddy (1986, pp. 247-263), Kumar et al. (2016, pp. 1755-1762), and Jenan et al. (2021, pp. 575-587) found that ionospheric irregularities occur during geomagnetic storms across various latitudes, particularly near the equator and lower latitudes. In these regions, the TEC within approximately ±20 degrees of the geomagnetic equator is higher, leading to greater disruptions in GNSS signal reception compared to other areas. Ionospheric behavior, classified into high, mid, and low latitudes as well as the equatorial region, is influenced by both solar and geophysical factors, resulting in TEC variations during geomagnetic storms (Hofmann-Wellenhof et al., 1992, pp. 1-134; Pi et al., 1997, pp. 2283-2286; Skone and de Jong., 2000, pp. 1067-1071; Chernyshov et al., 2020, pp. 1-13). These TEC anomalies contribute to signal delays, causing positional errors that range from a few meters to nearly 95-105 meters. Plasma density irregularities in the ionosphere distort electromagnetic wave propagation, leading to GNSS signal delays and disruptions in signal paths. The ionospheric layer is vast and exhibits variations in refractive index depending on the signal's operating frequency. To evaluate ionospheric delay, GPS L1 and L2 frequency signals are typically analyzed using frequency combinations and single-frequency ionospheric delay models. Several models have been proposed over the years to predict ionospheric delays, including those by Klobuchar (1986, pp. 280-286), Walker (1989, pp. 68-80), and Coster et al. (1992, pp. 191-204). However, despite advancements in modeling techniques, forecasting ionospheric conditions remains challenging due to the combined influence of terrestrial factors and space-based disturbances.

Several studies have investigated the impact of geomagnetic storms on GNSS performance. For example, Liu et al. (2010, pp. 795-805) analyzed TEC delays and their duration in response to geomagnetic disturbances. Kenpankho et al. (2011, pp. 365-370) compared TEC measurements with IRI models at equatorial latitudes, while Ratnam et al. (2011, pp. 1-6) examined ionospheric delay characteristics at low latitudes during geomagnetic storms. Kenpankho et al. (2013, pp. 1820-1826) further extended their research by comparing TEC measurements with IRI-2007 TEC in low-latitude and equatorial regions. Helmboldt et al. (2015, pp. 387-402) explored the effects of solar flares on the ionosphere at both local and hemispheric levels. Maggiolo et al. (2017, pp. 11,109-11,127) investigated the relationship between geomagnetic activity and delay time occurrences, particularly in connection with solar wind influences. Saito et al. (2017, pp. 1937-1947) analyzed ionospheric delays within Ground-Based Augmentation Systems (GBAS), while Zhang et al. (2018, pp. 1-15) focused on the impact of the ionosphere on GPS delay time. Pan and Guo (2018, pp. 1-17) expanded this research to include real-time delay issues across multiple GNSS systems, including GPS, GLONASS, Galileo, and BeiDou. Ansaria et al. (2019, pp. 248-258) examined TEC fluctuations and compared them with Auto-Regressive Moving Average (ARMA) models and Global Ionospheric Maps (GIM) over Japan. Zhang et al. (2020, pp. 1-16) studied the effects of geomagnetic storms on GPS signal loss in Taiwan. Marini-Pereira et al. (2020, pp. 1-16) mapped ionospheric delays in specific low-latitude regions, while Zhu et al. (2020, pp. 1-14) calibrated GNSS receiver delays using clock-steering characteristics. Sedeek (2020, pp. 1-15) investigated GPS TEC delays during geomagnetic storms over Egypt, and Zhang et al. (2021, pp. 1535-1545) reported TEC time delays during pre-storm and storm conditions in East Asia. Kenpankho et al. (2021, pp. 2152-2159) proposed real-time bias estimation methods for GPS receivers at low latitudes. Lastly, Zhbankov et al. (2022, pp. 194-201) examined the accuracy of satellite positioning systems affected by ionospheric conditions.

Based on data collection and a review of related research, Marini-Pereira et al. (2020, pp. 1-16) analyzed TEC delay maps in low-latitude regions. Their findings revealed that during periods of significant ionospheric activity, errors were typically below four meters in 99.99-100% of cases. On days with minimal ionization, the errors were generally less than one meter. Zhbankov et al. (2022, pp. 194-201) focused on the impact of ionospheric disturbances on GPS accuracy. Instead of relying on traditional techniques such as the Klobuchar model or TEC dependency values to correct ionospheric delays, they proposed a ray-tracing approach within a model designed to more accurately simulate real conditions. This method accounted for various types of Traveling Ionospheric Disturbances (TIDs). Their results demonstrated that large-scale TIDs could introduce errors ranging from 5 to 35 meters, whereas smaller-scale TIDs produced errors of less than two meters. Zhang et al. (2020, pp. 1-16) investigated GPS signal degradation during geomagnetic storms and identified a direct correlation between the maximum GPS signal loss at the receiver and the global average GPS signal's standard deviation. They employed the magnetic geography index to evaluate the severity of GNSS performance disruptions caused by geomagnetic storms. Kenpankho et al. (2021, pp. 2152-2159) examined bias in GPS TEC time delays by analyzing data from a GPS receiver located in a low-latitude region between 2004 and 2019. Their findings indicated that delay times at the receiver were significantly higher on disturbed days compared to calm days. For instance, the highest delay recorded on calm days was 5.8 ns, whereas on disturbed days, it reached up to 6.85 ns, with a minimum delay of 5.3 ns. Additionally, Keokhumcheng and Kenpankho (2025, pp. 4245-4259) compared TEC results obtained from single-frequency GPS with those from dual-frequency GPS, IGS TEC, and IRI TEC in 2023. Their results confirmed that TEC derived from a single-frequency GPS receiver is consistent and reliable for studying TEC delays in the ionosphere over the low-latitude region of Thailand.

After reviewing previous studies on the influence of ionospheric conditions on GPS signal delay, we conducted an investigation into GPS time delays at low latitudes, focusing on the intense geomagnetic storm that occurred on March 24, 2023, and April 24, 2023, over Chumphon, Bangkok and Chiang Mai, Thailand. During this event, significant ionospheric disturbances were observed, impacting satellite communications and GPS signal integrity. Our analysis involved identifying the highest and lowest GPS delay values recorded on the storm day. Additionally, we examined GPS delay times before and after the geomagnetic storm to assess its impact on signal delays, highlighting any significant variations.

II. METHODOLOGY

A. Method

For conducting this study, we utilized three datasets: geomagnetic storm data including planetary K-index (Kp) and disturbance storm time (Dst) indices, GPS TEC measurements from GNSS receiver equipment, and IGS TEC data. The IGS network of GPS receivers has been established, enabling consistent and regular observations. We focused on analyzing disruptions in the GPS delay time during severe (G4) geomagnetic storm that occurred on March 24, 2023, and April 24, 2023. The Space Weather Prediction Center (SWPC) reported the observation on severe geomagnetic storms in solar cycle 25. This event marked a significant geomagnetic storm in six years. Our investigation focused on analyzing GPS TEC data collected from a multi GNSS receiver station situated at low latitudes in Chumphon, Thailand. This specific location, known as the KMITL Chumphon station. The IGS TEC is collected by IGS Organization. This service, widely recognized as the International GPS Service (IGS), provides data from more than 500 stations all over the world. GPS data acquired from IGS centers are available in a Receiver Independent Exchange Format (RINEX) format. We collected all data and calculated GPS delay time during the period of the intense G4 geomagnetic storm, specifically from March 21, 2023, to March 29, 2023. The research methodology can be summarized as follows: Frist, we had data on severe geomagnetic storm event and categorized them based on physical indicators, including Kp and Dst indices. Second, IGS TEC data were obtained from IGS station at CPNM00THA, Chumphon, Thailand (10.725°N, 99.374°E). Then, GPS TEC raw data as RINEX files were received from GNSS receiver at KMITL Chumphon station, Thailand, (10.724°N, 99.375°E). Subsequently, we used the RINEX data to determine both of Slant Total Electron Content (STEC) and Vertical Total Electron Content (VTEC). Next, we calculated the GPS delay time. In conclusion, we conducted data analysis and provided a concise summary of our study findings.

B. Geomagnetic Storm

During the 25th solar cycle, the increase in solar activity and disturbances in the geomagnetic field resulted in the most severe geomagnetic storm in nearly six years. To facilitate data comparisons, a reference day was identified based on solar and geomagnetic conditions. Geomagnetic storm data were collected for the periods from March 21 to March 29, 2023, and April 21 to April 29, 2023. For a comprehensive analysis of GPS signal behavior, data were gathered over a nine-day span, including three days before the storm and five days following it. The primary focus of the analysis was on TEC irregularities and GPS signal delays. Hourly Dst index data can be accessed at: Kyoto WDC, while Kp index data are available at: NOAA SWPC. Additionally, hourly geomagnetic storm data for March 2023 can be retrieved from the IZMIRAN database at: IZMIRAN. The average intensity of the geomagnetic event was analyzed at hourly intervals using the Kp index as a reference.

C. GPS Data

The BG2 receiver is capable of receiving GPS satellite data at the KMITL station in Chumphon Province. Data from the THCP station (10.724°N, 99.375°E), THBK station (13.729°N, 100.775°E), and THCM station (18.771°N, 98.978°E) were analyzed for various types of observations. These include phase measurements for both L1 and L2 frequencies, as well as pseudo-range measurements using the C/A code on L1 (C1) and additional pseudo-range data on both L1 and L2 frequencies using the P code, labeled as P1 and P2, respectively. For this study, the focus was on observing and analyzing the signal quality and phase measurements on the L1 and L2 frequencies of GPS satellites. The data were sampled every 30 seconds. TEC values were derived from the slant path between the GPS satellite and the BG2 receiver, known as Slant Total Electron Content (STEC). The calculations for both L1 and L2 GPS frequencies were performed using the method and formula developed by Klobuchar (1996), with the resulting STEC values serving as variables for computing Vertical Total Electron Content (VTEC).

D. STEC

Each GPS satellite broadcasts signals at two distinct frequencies: f1 (1575.42 MHz) and f2 (1227.60 MHz). The receiver captures signals from 4 to 12 satellites, which are then used to STEC values. STEC, representing the electron content along the path from the satellite to the BG2s receiver, is calculated by determining the differences between P1 and P2 pseudo-ranges, as well as L1 and L2 phase differences, using Eq. (1) (Blewitt, 1990, pp. 199-202; Kenpankho et al., 2011, pp. 365-370; Keokhumcheng and Kenpankho, 2025, pp. 4245-4259).

$$\mathrm{STEC} = \frac{2(f_1 f_2)^2}{k(f_1^2 - f_2^2)}(L_1\lambda_1 - L_2\lambda_2) \quad (1)$$

where k is the related to the bending of signals due to ionospheric effects, 80.62 (m^3/s). λ_1 and λ_2 are the wavelengths with f_1 and f_2.

E. VTEC

VTEC refers to the TEC in a vertical orientation within a cross-sectional area of one square meter (Goodwin et al., 1995, pp. 1723-1732). It represents the TEC value at the point where the slant STEC intersects the ionosphere (Brunini et al., 2004, pp. 415-429). Therefore, VTEC can be considered equivalent to TEC, measured in electrons per square meter, and can be computed using the equation presented by Ma & Maruyama (2003, pp. 2083-2093), Kenpankho et al. (2011, p. 365-370), and Keokhumcheng and Kenpankho (2025, pp. 4245-4259) in Eq. (2).

$$\mathrm{VTEC} = \mathrm{STEC} \times \cos\chi \quad (2)$$

The zenith angle is defined as the angle measured from the vertical direction and is represented as χ.

$$\chi = \arcsin\left(\frac{R_E \cos\alpha}{R_E + h}\right) \quad (3)$$

where R_E is the radius of the Earth (6378 km). h is the altitude of the ionosphere layer (450 km).

F. GPS Delay Time

The GPS signal delay is calculated based on the electron density along the signal's propagation path and the corresponding carrier frequencies as

$$\Delta t = \frac{A}{cf^2} TEC \tag{4}$$

where A is the value of the refractive index of the medium.

$$\mathrm{A} = \frac{e^2}{8\pi^2 m\varepsilon_0} \tag{5}$$

where e is the electric charge (1.60217 x 10^{-19} C). m is the electron mass (9.109384 x 10^{-31} kg). ε_0 is the permittivity of free space (8.85419 x 10^{-12} F/m). A is 40.35.

$$\Delta t = \frac{1.34361\times10^{-7}}{f^2} TEC \tag{6}$$

GPS satellite signals are transmitted at f_1 = 1575.42 MHz and f_2 = 1227.60 MHz, which are defined as the primary frequencies for GPS communication.

$$\frac{1}{f^2} = \frac{1}{f_2^2} - \frac{1}{f_1^2} = \frac{f_1^2 - f_2^2}{f_1^2 f_2^2} = 2.6066\times10^{-19} \tag{7}$$

$$\Delta t = \frac{1.34361\times10^{-7}}{2.6066\times10^{-19}} TEC \tag{8}$$

$$\Delta t = 3.5023\times10^{-26} TEC \tag{9}$$

III. RESULTS

The analysis of GPS signal time delay for each event revealed significant variations influenced by geomagnetic activity. During intense geomagnetic storms, particularly on March 24, 2023 (Dst = -163 nT, Kp = 8) and April 24, 2023 (Dst = -213 nT, Kp = 8), the GPS signal delay times increased considerably, corresponding to fluctuations in TEC as follows.

A. GPS signal delay in Thailand event on March 24, 2023

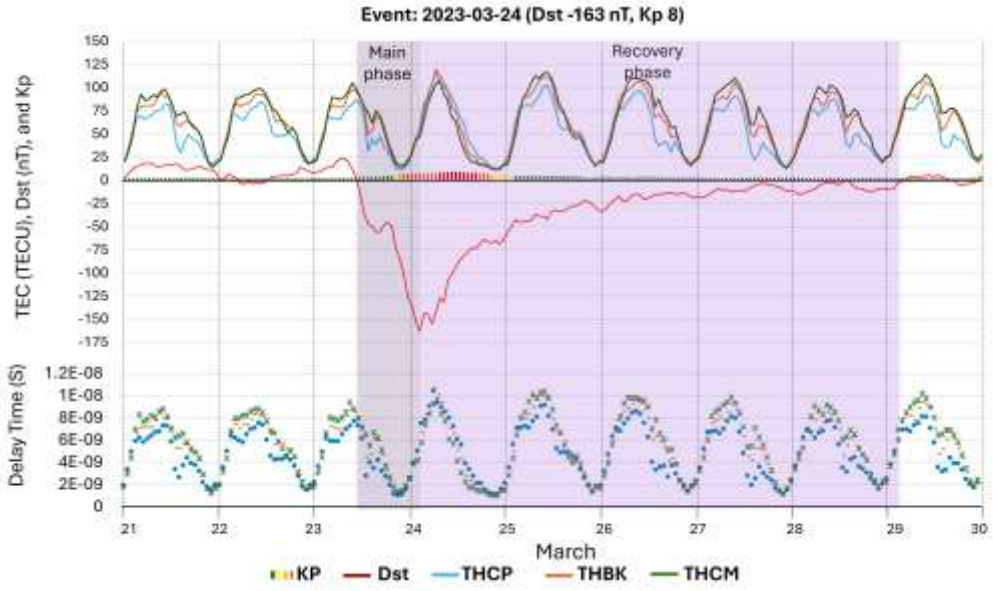

Figure 1: Analysis of the G4 Geomagnetic Storm (Dst = -163 nT, Kp = 8) on TEC and GPS signal delay in Thailand event on March 24, 2023.

This graph in Figure 1 presents an analysis of TEC, the Dst index, the Kp index, and GPS signal delay time during the geomagnetic storm event on March 24, 2023. Classified as a strong geomagnetic storm (Dst = -163 nT, Kp = 8), this event significantly impacted ionospheric conditions and GNSS signal propagation. The x-axis represents the time period from March 21 to March 29, 2023, covering the pre-storm, storm, and post-storm phases. The event is divided into two key phases: the main phase (March 24), where a significant geomagnetic disturbance occurred, and the recovery phase (March 25-29), during which the ionosphere gradually returned to normal conditions. The left y-axis displays TEC values from three GNSS stations THCP (Chumphon, blue line), THBK (Bangkok, orange line), and THCM (Chiang Mai, green line) along with the Dst index (red line), which represents global geomagnetic activity, showing a sharp drop to -163 nT on March 24, indicating a strong storm. The Kp index reflects the intensity of the storm, reaching Kp 8, signifying severe geomagnetic activity. The right y-axis illustrates GPS signal delay times (in seconds), with the lower part of the graph showing delay variations for the three GNSS stations. The delay times increased significantly during the storm, peaking on March 24, and gradually decreased as the ionosphere recovered. The TEC values exhibit daily variations, with peaks during the daytime and lower values at night. Before the storm, TEC shows a sharp increase, followed by significant fluctuations during and after the event. The Dst index reveals a negative spike at -163 nT, marking the onset of the geomagnetic storm, which corresponds to the most significant TEC disturbances and GPS signal delays. GPS signal delays fluctuate daily, closely aligning with TEC variations, and are more pronounced at lower latitudes at stations THCP (10.43 ns) and THBK (10.70 ns), where ionospheric disturbances are stronger. Overall, this graph highlights the substantial impact of geomagnetic storms on TEC and GPS signal delays, with the March 24, 2023, event causing significant ionospheric disturbances, as evidenced by a sharp drop in Dst (-163 nT), a high Kp index (8), and noticeable fluctuations in TEC and GPS delays at all three stations. These findings emphasize the strong influence of geomagnetic storms on GNSS-based applications, particularly in low-latitude regions like Thailand, where ionospheric disturbances tend to be more severe.

B. GPS signal delay in Thailand event on April 24, 2023

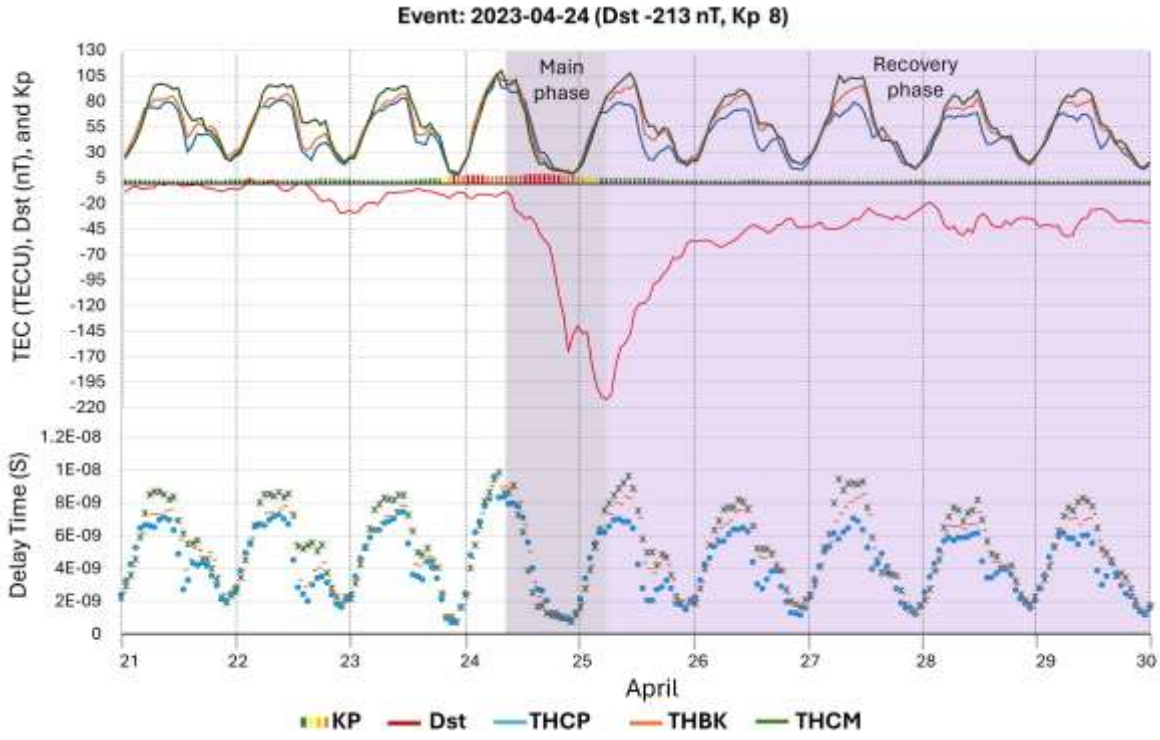

Figure 2: Analysis of the G4 Geomagnetic Storm (Dst = -213 nT, Kp = 8) on TEC and GPS signal delay in Thailand event on April 24, 2023.

This graph in Figure 2 illustrates the analysis of TEC, the Dst index, the Kp index, and GPS signal delay time during the geomagnetic storm event on April 24, 2023. Classified as a strong geomagnetic storm (Dst = -213 nT, Kp = 8), this event significantly impacted ionospheric conditions and GNSS signal propagation. The x-axis represents the time period from April 21 to April 29, 2023, covering the pre-storm, storm, and post-storm phases. The storm is divided into two key phases: the main phase (April 24), characterized by a sharp negative spike in the Dst index (-213 nT) indicating severe geomagnetic disturbance, and the recovery phase (April 25–29), during which the ionosphere gradually returned to normal conditions. The left y-axis displays TEC values from three GNSS stations THCP (Chumphon, blue line), THBK (Bangkok, orange line), and THCM (Chiang Mai, green line) alongside the Dst index (red line) and the Kp index, which reached a maximum value of Kp 8, signifying intense geomagnetic activity. The right y-axis represents GPS signal delay times (in seconds), where the lower section of the graph shows significant variations in delay times at the three GNSS stations. The delay times increased notably during the storm, peaking on April 24, before gradually decreasing as the ionosphere recovered. TEC values exhibit regular daily variations, peaking during the daytime and decreasing at night, with a sharp decrease during the main phase, indicating ionospheric disturbances. GPS signal delays show a strong correlation with TEC fluctuations, particularly at lower latitudes stations THCM (9.85 ns), THCP (9.59 ns), and THBK (9.56 ns), where ionospheric disturbances are more pronounced. Overall, this graph highlights the significant impact of the April 24, 2023, geomagnetic storm on TEC and GPS signal delays, reinforcing the strong influence of geomagnetic activity on GNSS-based applications, especially in low-latitude regions like Thailand, where ionospheric effects are more intense.

IV. DISCUSSION

The results of this study indicate that TEC values increase during geomagnetic storms compared to the periods before and after the storm, a pattern that aligns with previous findings by Liu et al. (2010, pp. 795-805), Kenpankho et al. (2011, pp. 365-370), Ratnam et al. (2011, pp. 1-6), Kenpankho et al. (2013, pp. 1820-1826), Helmboldt et al. (2015, pp. 387-402), Ansaria et al. (2019, pp. 248-258), Sedeek (2020, pp. 1-15), Zhang et al. (2021, pp. 1535-1545), and Zhbankov et al. (2022, pp. 194-201). Additionally, the impact of geomagnetic storms on TEC variations is consistent with observations by Maggiolo et al. (2017, pp. 11,109-11,127), Saito et al. (2017, pp. 1937-1947), Zhang et al. (2018, pp. 1-15), Pan and Guo (2018, pp. 1-17), Zhang et al. (2020, pp. 1-16), Zhu et al. (2020, pp. 1-14), Sedeek (2020, pp. 1-15), Zhang et al. (2021, pp. 1535-1545), and Kenpankho et al. (2021, pp. 2152-2159), all of whom reported significant TEC fluctuations associated with geomagnetic disturbances. Furthermore, the observed TEC variations closely follow the trends described by Keokhumcheng and Kenpankho (2025, pp. 4245-4259), who demonstrated that TEC values exhibit substantial fluctuations in response to geomagnetic activity, particularly in low-latitude regions. The findings from this study confirm that geomagnetic storms contribute to significant ionospheric disturbances, leading to increased GPS signal delays, further supporting the notion that TEC variations play a crucial role in affecting GNSS-based applications, particularly in low-latitude regions like Thailand, where ionospheric effects tend to be more pronounced. These results underscore the necessity of continuous ionospheric monitoring and the development of enhanced models to mitigate the adverse impacts of geomagnetic storms on satellite-based navigation and communication systems.

V. CONCLUSION

This study confirms that GPS signal delay increases significantly during intense geomagnetic storms, particularly in low-latitude regions like Chumphon, Bangkok, and Chiang Mai, Thailand. The results show that on March 24, 2023, and April 24, 2023, the GPS signal delay was notably higher compared to quiet days, aligning with the findings of Kenpankho et al. (2021, pp. 2152-2159), who analyzed GPS receiver delay in the same region from 2004 to 2019 and reported that delays were consistently higher on disturbed days. While GPS delay on quiet days ranged between 4.25 and 5.75 ns, it increased to 5.25-6.85 ns during geomagnetic storms. In this study, during the March 24, 2023, storm, the delay peaked at 0.1 ns and dropped between 38 and 40 ns, before gradually returning to normal levels after the storm, with a maximum of 0.25-0.3 ns and a minimum of 49-50 ns. Furthermore, these findings are consistent with the research of Keokhumcheng and Kenpankho (2025, pp. 4245-4259), which emphasized the significant impact of TEC variations in the ionosphere over low-latitude regions such as Chumphon Province. Overall, this study reinforces the strong correlation between geomagnetic activity, TEC fluctuations, and GPS signal delay, highlighting the need for continuous monitoring and improved ionospheric models to enhance GNSS accuracy, particularly in low-latitude regions prone to ionospheric disturbances.

ACKNOWLEDGEMENT

This research was completed with the cooperation of multiple organizations. We would like to express our gratitude to the Institute of Geology and Geophysics, Chinese Academy of Sciences (IGGCAS), and the Earthquake Observation Division (EOD), Thai Meteorological Department (TMD), for their support in providing the BG2 GNSS receiver and for their valuable guidance in this study. We also appreciate IRI and IGS for providing TEC data used for TEC validation, as well as the Space Weather Prediction Center (SWPC) of the National Oceanic and Atmospheric Administration (NOAA) for geomagnetic storm activity data. We would like to express our gratitude to IZMIRAN for supplying the hourly geomagnetic storm data along with the Kp indices. Additionally, we appreciate the World Data Center (WDC) for Geomagnetism in Kyoto, Japan, for providing the

Dst index data. Lastly, we extend our sincere appreciation to the Space Satellite Study Laboratory (SSS Lab), School of Industrial Education and Technology (SIET), King Mongkut's Institute of Technology Ladkrabang (KMITL), for their support in providing equipment and facilities for data collection.

REFERENCES

Ansari, K., Park, K.-D., & Kubo, N. (2019). Linear time-series modeling of the GNSS based TEC variations over Southwest Japan during 2011–2018 and comparison against ARMA and GIM models. *Acta Astronautica, 165*, 248-258.

Blewitt, G. (1990). An automatic editing algorithm for GPS data. *Geophysical Research Letters, 17*(3), 199-202.

Brunini, C., Meza, A., Azpilicueta, F., Van Zele, M. A., Gende, M., & Díaz, A. (2004). A new ionosphere monitoring technology based on GPS. *Astrophysics and Space Science, 290*, 415-429.

Chernyshov, A. A., Miloch, W. J., Jin, Y., & Zakharov, V. I. (2020). Relationship between TEC jumps and auroral substorm in the high-latitude ionosphere. *Scientific Reports, 10*(1), 1-13.

Chinmaya, N., Tsai, L. C., Su, S. Y., & Galkin, I. A. (2016). Peculiar features of the low-latitude and mid-latitude ionospheric response to the St. Patrick's Day geomagnetic storm of 17 March 2015. *Journal of Geophysical Research: Space Physics, 121*(8), 7941-7960.

Coster, A. J., Gaposchkin, E. M., & Thornton, L. E. (1992). Real-time ionospheric monitoring system using GPS. *Navigation, 39*(2), 191-204.

Goodwin, G. L., Silby, J. H., Lynn, K. J. W., Breed, A. M., & Essex, E. A. (1995). GPS satellite measurements: Ionospheric slab thickness and total electron content. *Journal of Atmospheric and Terrestrial Physics, 57*(14), 1723-1732.

Helmboldt, J. F., Kassim, N. E., & Teare, S. W. (2015). Observations of the ionospheric impact of M-class solar flares on local and hemispheric scales. *Earth and Space Science, 2*(10), 387-402.

Hofmann-Wellenhof, B., Lichtenegger, H., & Collins, J. (1992). *GPS -Global positioning system: Theory and practice* (4th ed.). Springer -Verlag wien.

Jenan, R., Dammalage, T. L., & Panda, S. K. (2021). Ionospheric total electron content response to September-2017 geomagnetic storm and December-2019 annular solar eclipse over Sri Lankan region. *Acta Astronautica, 180*, 575-587.

Kenpankho, P., Chaichana, A., Trachu, K., Supnithi, P., & Hozumi, K. (2021). Real-time GPS receiver bias estimation. *Advances in Space Research, 68*(5), 2152-2159.

Kenpankho, P., Supnithi, P., & Nagatsuma, T. (2013). Comparison of observed TEC values with IRI-2007 TEC and IRI-2007 TEC with optional foF2 measurements predictions at an equatorial region, Chumphon, Thailand. *Advances in Space Research, 52*(10), 1820-1826.

Kenpankho, P., Watthanasangmechai, K., Supnithi, P., Tsugawa, T., & Maruyama, T. (2011). Comparison of GPS TEC measurements with IRI TEC prediction at the equatorial latitude station, Chumphon, Thailand. *Earth, Planets and Space, 63*, 365-370.

Keokhumcheng, T., & Kenpankho, P. (2025). The study of total electron content on ionosphere by using single frequency GPS receiver. *Advances in Space Research, 75*(5), 4245-4259.

Klobuchar, J. A. (1986). Design and Characteristics of the GPS ionospheric time delay algorithm for single frequency users. Proceedings of the PLANS-86 conference, 280-286, New York, Institute of Electrical and Electronic Engineers, Las Vegas, NV.

Kumar, K. V., Maurya, A. K., Kumar, S., & Singh, R. (2016). 22 July 2009 total solar eclipse induced gravity waves in ionosphere as inferred from GPS observations over EIA. *Advances in Space Research, 58*(9), 1755-1762.

Liu, J., Zhao, B., & Liu, L. (2010). Time delay and duration of ionospheric total electron content responses to geomagnetic disturbances. *Annales Geophysicae, 28*(3), 795-805.

Ma, G., & Maruyama, T. (2003). Derivation of TEC and estimation of instrumental biases from GEONET in Japan. *Annales Geophysicae, 21*(10), 2083-2093.

Maggiolo, R., Hamrin, M., De Keyser, J., Pitkänen, T., Cessateur, G., Gunell, H., & Maes, L. (2017). The delayed time response of geomagnetic activity to the solar wind. *Journal of Geophysical Research: Space Physics, 122*(11), 11,109-11,127.

Marini-Pereira, L., Lourenço, L. F. D., Sousasantos, J., Moraes, A. O., & Pullen, S. (2020). Regional ionospheric delay mapping for low-latitude environments. *Radio Science, 55*(12), 1-16.

Pan, L., & Guo, F. (2018). Real-time tropospheric delay retrieval with GPS, GLONASS, Galileo and BDS data. *Scientific Reports, 8*(1), 1-17.

Pi, X., Mannucci, A. J., Lindqwister, U. J., & Ho, C. M. (1997). Monitoring of global ionospheric irregularities using the worldwide GPS network. *Geophysical Research Letters, 24*(18), 2283-2286.

Ratnam, D. V., Sarma, A. D., Srinivas, V. S., & Sreelatha, P. (2011). Performance evaluation of selected ionospheric delay models during geomagnetic storm conditions in low-latitude region. *Radio Science, 46*(03), 1-6.

Reddy, C. A. (1986). The equatorial ionosphere. *Indian Journal of Radio & Space Physics, 15*(5&6), 247-263.

Reddybattula, K. D., Panda, S. K., Ansari, K., & Peddi, V. S. R. (2019). Analysis of ionospheric TEC from GPS, GIM and global ionosphere models during moderate, strong, and extreme geomagnetic storms over Indian region. *Acta Astronautica, 161*, 283-292.

Saito, S., Sunda, S., Lee, J., Pullen, S., Supriadi, S., Yoshihara, T., Terkildsen, M., Lecat, F., & ICAO APANPIRG Ionospheric Studies Task Force. (2017). Ionospheric delay gradient model for GBAS in the Asia-Pacific region. *GPS Solutions, 21*, 1937-1947.

Sedeek, A. (2020). Ionosphere delay remote sensing during geomagnetic storms over Egypt using GPS phase observations. *Arabian Journal of Geosciences, 13*(811), 1-15.

Serafimov, K. B., Arshinkov, I. S., Bochev, A. Z., Petrunova, M. H., Stanev, G. A., & Chapkanov, S. K. (1982). A measuring equipment for electric and magnetic fields in the range of the ionosphere-Magnetosphere plasma mounted aboard the “Intercosmos-Bulgaria 1300” satellite. *Acta Astronautica, 9*(6-7), 397-399.

Skone, S., & de Jong, M. (2000). The impact of geomagnetic substorms on GPS receiver performance. *Earth, Planets and Space, 52*, 1067-1071.

Verkhoglyadova, O., Maus, N., & Meng, X. (2021). Classification of high density regions in global ionospheric maps with neural networks. *Earth and Space Science, 8*(7), 1-12.

Walker, J. K. (1989). Spherical cap harmonic modelling of high latitude magnetic activity and equivalent sources with sparse observations. *Journal of Atmospheric and Terrestrial Physics, 51*(2), 67-80.

Zhang, Z., Guo, F., & Zhang, X. (2018). The effects of higher-order ionospheric terms on GPS tropospheric delay and gradient estimates. *Remote Sensing, 10*(10), 1-15.

Zhang, S., He, L., & Wu, L. (2020a). Statistical study of loss of GPS signals caused by severe and great geomagnetic storms. *Journal of Geophysical Research: Space Physics, 125*(9), 1-16.

Zhang, Y., Wu, Z., Feng, J., Xu, T., Deng, Z., & Zhen, W. (2020b). Statistical study of the time delay of ionospheric TEC storms to geomagnetic storms in Taoyuan, Taiwan. *Advances in Space Research, 65*(1), 86-94.

Zhang, Y., Wu, Z., Feng, J., Xu, T., Deng, Z., Ou, M., & Xiong, W. (2021). Time delay of ionospheric TEC storms to geomagnetic storms and pre-storm disturbance events in East Asia. *Advances in Space Research, 67*(5), 1535-1545.

Zhbankov, G. A., Danilkin, N. P., & Maltseva, O. A. (2022). Influence of the ionosphere on the accuracy of the satellite navigation system. *Acta Astronautica, 190*, 194-201.

Zhu, F., Zhang, H., Huang, L., Li, X., & Feng, P. (2020). Research on absolute calibration of GNSS receiver delay through clock-steering characterization. *Sensors, 20*(21), 1-14.